Relation Between Molecular Orientation and Mechanical Properties in Differently Processed Polyamide 4.6/6 Textile Yarns

G. SCHMACK,[1] R. SCHREIBER,[2] W. S. VEEMAN,[2] H. HOFMANN,[1] R. BEYREUTHER[1]

[1] Institute of Polymer Research Dresden, Department opf Fiber Formation, Hohe Strasse 6, 01069 Dresden, Germany

[2] Department of Physical Chemistry, University of Duisburg, Germany

Received 9 December 1996; accepted 7 March 1997

ABSTRACT: A series of Polyamide 4.6/6 textile fibers spun according to different technologies, high-speed spinning, and the spin drawing, was investigated by ^{13}C-NMR, ultrasonic, optical, WAXS, and DSC measurements. It was shown from the determination of the chain orientational order parameters and the DSC results that in the as-spun textile fibers two different crystallization modes occur, i.e., up to spinning speeds of 3500 m/min spherulites and orientationally ordered crystallites are present at the same time. With increasing fiber spinning speeds, the orientationally ordered crystallites grow at the expense of the spherulitic structures. At spinning speeds beyond 3500 m/min the spherulites vanish completely and only the orientationally ordered crystallites are observable and the tenacity increases. The drawn fibers only show a fibril-like structure and spherulites do not occur. Accordingly the drawn fibers have a higher level of tenacity. © 1997 John Wiley & Sons, Inc. J Appl Polym Sci **66:** 377–385, 1997

Key words: PA 4.6/6-fibers; ^{13}C-NMR; DSC; ultrasonic measurements; orientational order parameter

INTRODUCTION

Polyamide 4.6 (PA 4.6) is an engineering polymer (Stanyl™) produced by DSM. For yarns and technical fibers a copolymer with 5% caprolactam is used, leading to PA 4.6/6.[1] These materials offer attractive properties because of their high melting temperature, heat capacity, crystallization rate, degree of crystallinity, and dimensional stability.[2] This combination of properties is responsible for a structure formation, which differs from that of PA 6 and PA 6.6.

Target applications are technical yarns for sewing threads, airbags, mechanical rubber goods, tire cords, and abrasion resistant fabrics as well as textile and carpet yarns.[3]

DSC, TEM, ultrasonic, optical, WAXS, and NMR studies[4,5] have been done on PA 4.6/6 yarns, which were spun by means of two different technologies, high-speed spinning and spin drawing. These technologies lead to a variation in process conditions and cause changes in crystallinity, morphology, and molecular orientation. The main emphasis of this report is the relation between the chain orientation and the crystalline structure induced by the spinning process.

EXPERIMENTAL

The fiber grade, Stanyl TS 611, used in this study, has been provided by DSM.

Correspondence to: G. Schmack.
Dedicated to Prof. Dr. H.-J. Jacobasch on his 60th birthday.
Contract grant support: DSM Management.

Journal of Applied Polymer Science, Vol. 66, 377–385 (1997)
 CCC 0021-8995/97/020377-09

The intrinsic viscosity of the granulate was 2.66 dL/g, measured in a solution of 1 g PA 4.6/6 in 100 mL sulfuric acid (96%) at 25°C. The fibers were spun using a spinning equipment of the Institute of Polymer Research Dresden. A geometry commonly used for polyamide was chosen for the extruder screw. The conditions of extrusion (temperature profile) were adapted according to the higher spinning temperature of PA 4.6/6 of 300 ± 3°C. The residence time of the polymer melt in the extruder was about 2 min. The geometry of the single spinneret was 0.35 × 0.70 mm obtaining yarns with 24 filaments.

In the high-speed spinning process the fibers (partially oriented yarns, POYs) were spun at a constant throughput of 44 g/min. The take-up velocities were in the range of 2000–5000 m/min. In the spin-drawing process the fibers (fully drawn yarns, FDYs) were spun at about 600 m/min and drawn between heated godets in two steps.

The draw ratios for the FDYs were chosen in a way that the elongation was constant at about 15%.

The melting enthalpy was determined by Differential Scanning Calorimetry (DSC) using a Perkin–Elmer calorimeter (DSC 7). The temperature was increased 50 to 315°C at a heating rate of 10 K/min. The measurements were carried out under nitrogen flow.

The crystalline orientation was determined by Eltink[5] from the Statton flat film WAXS pattern using Ni filtered Cu K_α radiation at 50 kV and 40 mA.

The measurements of birefringence were carried out using a polarizing microscope and an Ehringhaus twin compensator.

The propagation velocity v_v of an acoustic pulse wave front through the yarn was determined by the SLM-1 measurement system from Ilse Elektrotechnik. The measuring frequency was 10 MHz. The measuring distance on the filament was 30 cm.

The morphological investigations were carried out by means of Transmission Electron Microscopy (TEM). The sections were prepared by cryo ultrathin sectioning technique parallel to the fiber axis and stained with OsO_4 and RuO_4.

The stress–strain tests were done on an Instron Universal Tester TF-CM. The two-dimensional rotor-synchronized ^{13}C-MAS NMR experiments were performed on a Bruker ASX 400 Spectrometer, operating at 100.63 MHz for ^{13}C. Spinners of 7 mm diameter were used in a double bearing CP/MAS probehead. The spinning frequency was 2000 Hz and a proton 90° pulse of 5 μs was applied. The recycle delay was 2 s and the crosspolarization mixing time 1 ms. Adamantane was used to optimize the Hartmann–Hahn condition. The evolution time t_1 was incremented with $\frac{1}{16}$ of the rotor period.

The fibers for the NMR orientation measurements were wound in a parallel fashion and glued with water glass into a flat layer. Four to five of these layers were glued together and a block of 4 × 4.5 × 11 mm was cut in such a way that the fiber draw direction and the long block axis formed an angle of 60° (angle β_1 in Fig. 1). The block was mounted in the rotor with its long axis parallel to the rotor axis. The space between rotor and the block was filled with talcum in order to ensure stable spinning. The samples are shown in Table I.

Theory

The Rotorsynchronized 2D-CP/MAS Experiment

If an oriented sample is placed into the magic angle rotor in such a way that the rotor axis and the order axis of the sample form an angle β_1 (Fig. 1), which is not equal to zero, the 1D-MAS spectrum is dependent on the rotor phase γ_1 at the beginning of the rf pulsing. This is caused by the anisotropy of the magnetic shielding tensor.

The higher the orientational order of the sample, the stronger the dependence of the spectrum on the rotor phase. Therefore, an unoriented sample does not show any rotor phase dependency. By the rotorsynchronized two-dimensional ^{13}C-MAS experiment of Harbison and Spiess,[6,7] a two-dimensional NMR spectrum consisting of a row of one-dimensional spectra (slices) is obtained. The two-dimensional spectrum formed by the slices contains the ^{13}C chemical shift information in the F_2 dimension and the orientation information in the F_1 dimension.

The Order Parameters

The line intensities in the two-dimensional ^{13}C spectrum were fitted with a theoretical spectrum calculated by an orientation distribution function (ODF) $f(\theta)$, expanded in Legendre polynomials:

$$f(\theta) = \sum_L (2L + 1) \langle P_L \rangle P_L(\cos \theta)$$

where L can take even values only. It is assumed, that the chains in the fibers are distributed randomly around the fiber axis and that the mole-

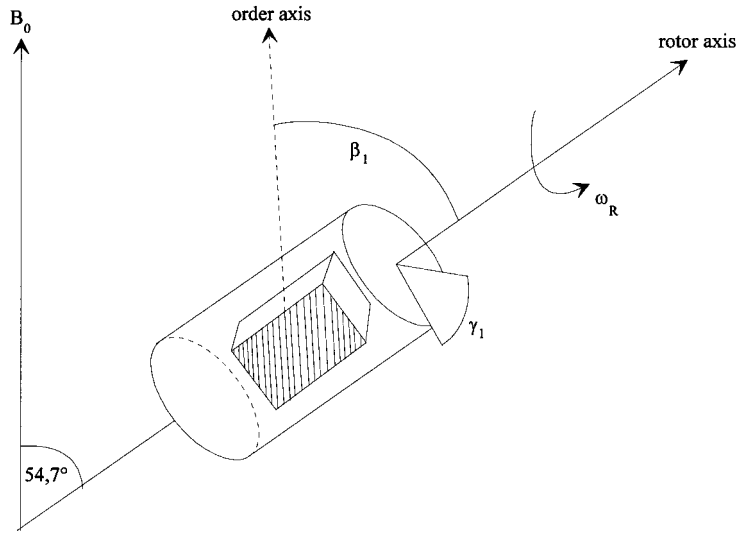

Figure 1 Scheme of the rotorsynchronized MAS experiment with definition of angle β_1 and the rotor phase γ_1.

cules are distributed randomly around the chain axis. Therefore, the system possesses axial symmetry and only one angle θ is needed to define the ODF $f(\theta)$.

The order parameters $\langle P_L \rangle$ represent the weighing factors, with which the Legendre polynomials contribute to the orientation distribution function:

$$\langle P_L \rangle = \int_0^{\pi} P_L(\cos\theta) f(\theta) \sin\theta \, d\theta.$$

The order parameters can vary from 0 for completely unoriented to 1 for completely oriented samples. The ODF $f(\theta)$ is completely defined when all the moments $\langle P_L \rangle$ of the expansion are known. The expansion coefficients, the order parameters $\langle P_L \rangle$, are determined by a least square-fitting procedure. Together with the order parameters the principal values of the ^{13}C chemical shift tensor are obtained also.[8] By most experiments only a few order parameters $\langle P_L \rangle$ can be determined. Birefringence leads only to the value of $\langle P_2 \rangle$, the sonic modulus leads to $\langle P_2 \rangle$ and $\langle P_4 \rangle$.[9] Theoretically, the number of order parameters $\langle P_L \rangle$ that can be determined with NMR is unlimited. In practice, the number is limited by the spectral signal-to-noise ratio. The higher the orientational order, the more order parameters can be determined.

Table I The Samples With Their Take-Up Velocity v and the Draw Ratio λ

Yarn	v (km/min)	λ
POY	2.0	
POY	2.5	
POY	3.0	
POY	3.5	
POY	4.0	
POY	4.5	
POY	5.0	
FDY	0.6	4.5

The most commonly used order parameter, $\langle P_2 \rangle$, characterizes the width of the ODF, the smaller the value, the broader the orientation distribution. When the order parameters do not converge rapidly, even the knowledge of $\langle P_2 \rangle$, $\langle P_4 \rangle$, and $\langle P_6 \rangle$ does not guarantee accurate knowledge of the ODF.

Because the Legendre polynomials are orthogonal, the value of $\langle P_2 \rangle$ should not depend on the fact whether the higher order parameters are known. The values of the order parameter $\langle P_2 \rangle$, determined via different techniques, can therefore directly be compared.

When comparing order parameters determined via different techniques, another consideration is what part of the molecule and of the sample contributes to the measured order parameters. The rotation-synchronized ^{13}C-MAS NMR technique used in this report is a clear example for this, while only the carbonyl resonance is employed for the order parameter determination. The CH_2 resonances overlap too much. For the sonic experi-

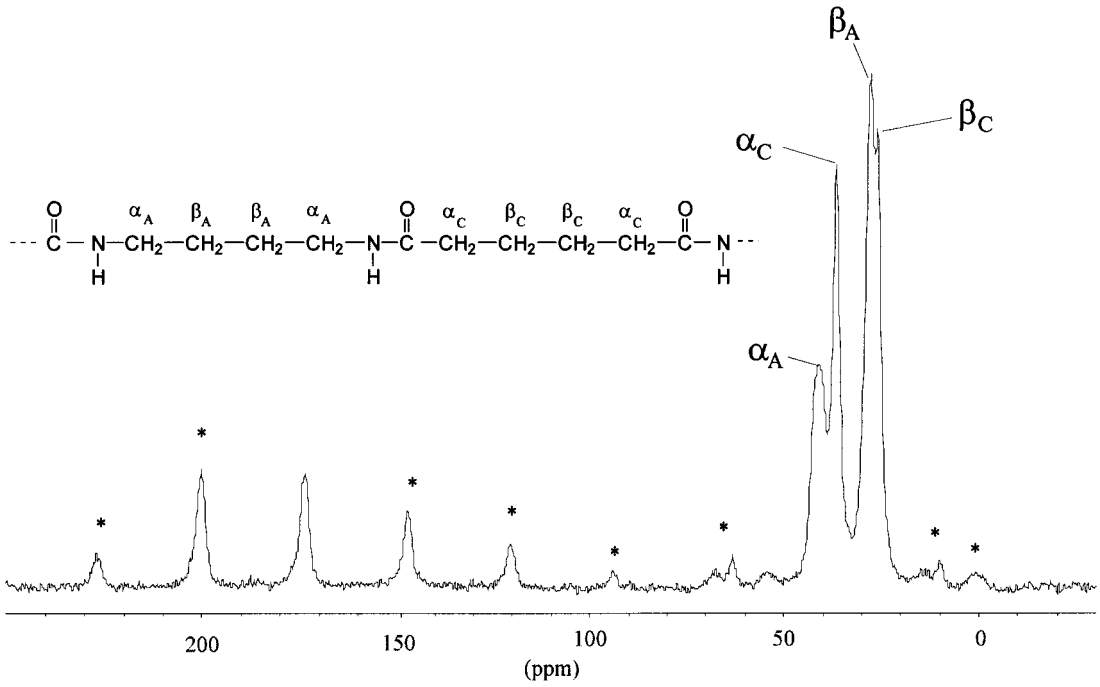

Figure 2 ^{13}C-CPMAS spectrum of a fiber spun in the high-speed spinning process with a speed of 5000 m/min. The rotor frequency was 2000 Hz. Spinning sidebands are marked with asterisks.

ments the whole molecule contributes to the measured order parameters. Another complication is the presence of crystalline and amorphous regions. Although, in principle, NMR has the possibility to differentiate between contributions from crystalline and amorphous domains, this has not been tried for these samples yet.

RESULTS

NMR

Figure 2 shows the CPMAS ^{13}C spectrum of a sample spun at 5000 m/min and the assignment of the peaks. The rotorsynchronized 2D-CP/MAS spectrum of a fiber spun at 5000 m/min is shown in Figure 3. With increasing spinning speed signals in higher slices were obtained. This indicates that the orientation in the fibers increases with increasing spinning speeds. For the determination of the order parameters only the carbonyl resonances were exploited, because the CH_2-peaks overlap too much. The experimentally determined order parameters, which are the mean value of the crystalline and amorphous fractions, and ^{13}C chemical shift tensor values are listed in Table II.

At increasing spinning speed the $\langle P_2 \rangle$ values increase linearly, which corresponds to a narrower orientation distribution around the order axis. The higher the degree of orientation the more order parameters can be determined. For the most oriented sample (POY, 5000 m/min) order parameters up to $\langle P_6 \rangle$ were obtained.

TEM Micrographs

The TEM-pictures of slices parallel to the fiber axis indicate that there are spherulitic structures inside the POYs spun at low velocities ($<$3500 m/min). The spherulites start to deform in the direction of the filament axis already at a speed of 3000 m/min (Fig. 4). At velocities above 3500 m/min spherulitic structures can not be found in the POYs anymore. The FDYs, on the other hand, show a fibril-like structure (Fig. 5).

DSC

The thermograms of the POYs spun at different velocities are shown in Figure 6 in a small temperature range. Two melting peak maxima are visible for POYs spun between 2000 and 3500 m/min. This indicates that there are two different crystal-

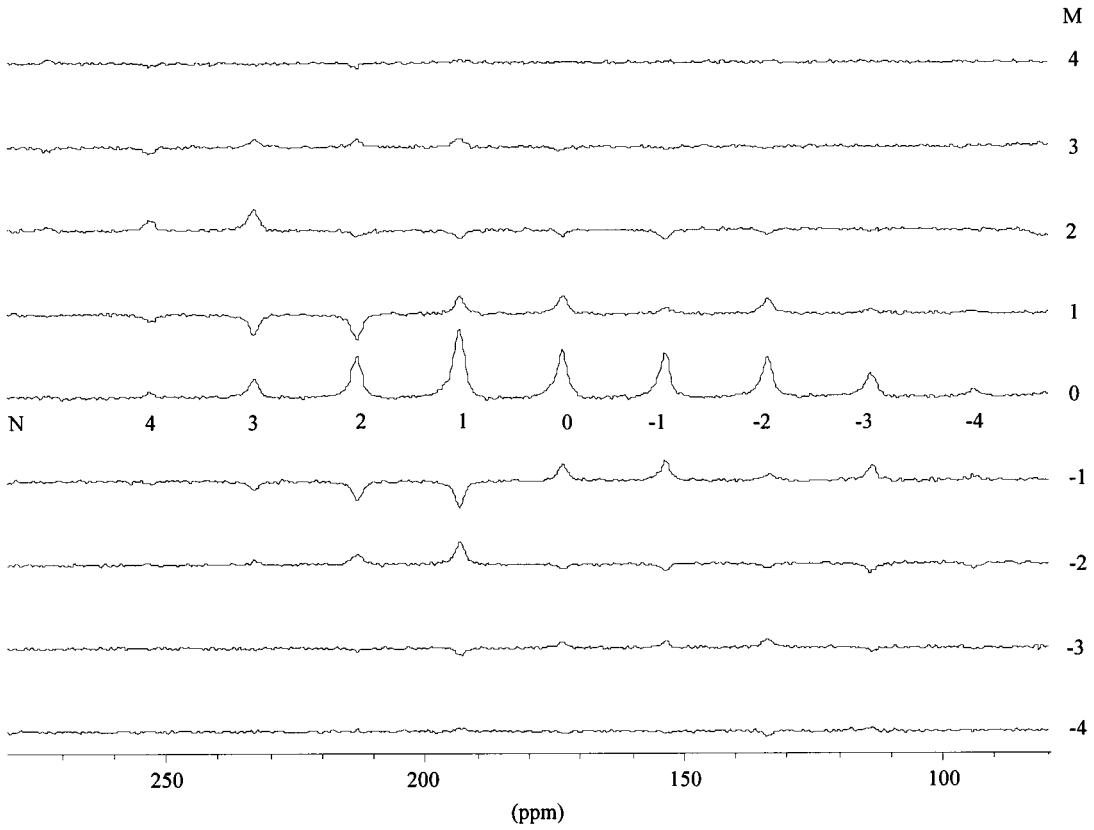

Figure 3 Rotorsynchronized 2D-CP/MAS spectrum of a fiber spun at 5000 m/min.

line regions in these fibers. One region has got relatively unstable crystallites, which are reorganized in dependence on the heating rate in the DSC and melt in a second peak. The area of the second peak decreases at increasing spinning speed and vanishes completely, if the fibers are spun at velocities higher than 3500 m/min. The crystallites are more orientionally ordered and the area of the first melting peak increases and is shifted to higher temperatures.

Pulse Propagation Measurements

According to Dumbleton[10] the sonic moduli ($E = v_v^2 \gamma$) can be expressed in terms of the orientations of the crystalline and amorphous regions,

$$\frac{3}{2}\left(\frac{1}{E_u - E_{or}}\right) = \frac{x f_c}{E_c^\circ} + \frac{(1-x) f_a}{E_a^\circ}$$

$$\frac{3}{2}\left(\frac{1}{E_u}\right) = \frac{x}{E_c^\circ} - \frac{1-x}{E_a^\circ}$$

where E_u is the modulus for an unoriented fiber and E_{or} is the modulus in the orientation direction, x is the degree of crystallinity, f_c and f_a are the order parameters, and E_c° and E_a° are the transverse Young's moduli for the crystalline and amorphous region, respectively.

The transverse Young's moduli were obtained from an unoriented fiber spun at a low velocity

Table II Order Parameters and Chemical Shift Principal Values, Determined by Fitting the Peak Intensities in the Rotation-Synchronized 2D-MAS Experiment of Three POY Samples

	^{13}C Principal Values			Order Parameters		
POY	σ_{11}	σ_{22}	σ_{33}	$\langle P_2 \rangle$	$\langle P_4 \rangle$	$\langle P_6 \rangle$
5000 m/min	−238.7	−186.1	−96.3	0.73	0.51	0.33
3500 m/min	−241.7	−185.1	−94.3	0.59	0.22	—
2000 m/min	−239.7	−185.1	−96.3	0.45	—	—

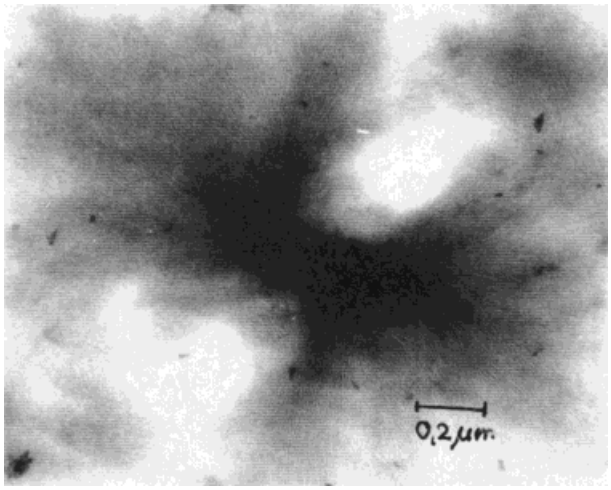

Figure 4 TEM micrograph of a fiber spun at 3000 m/min, (60,000 : 1).

(100 m/min). This fiber was prepared by a relaxed annealing treatment to obtain different crystalline parts. The extrapolation of the graph of $1/E_u$ vs. x (with $x = 1$ and $x = 0$) gives the following results: $E_a^\circ = 1.51$ GPa and $E_c^\circ = 2.95$ GPa. It can also be seen that a linear extrapolation from E_{or} to zero winding speed agrees within the margin of error with the value of E_a° for unoriented samples.

The overall crystalline volume fraction x was determined by DSC measurements: $x = \Delta H/\Delta H_o$. The value of the melting heat of PA 4.6 for a crystal of infinite thickness was calculated by Hong[11] to $\Delta H_o = 270$ J/g. For the copolymer PA 4.6/6 with 5% caprolactam, a value of $\Delta H_o = 257$ J/g was assumed.

The overall density γ was calculated by means of the crystalline volume fraction x.

$$\gamma = (1 - x)\gamma_a + x\gamma_c.$$

The amorphous and crystalline densities $\gamma_a = 1.15$ g/cm^3 and $\gamma_c = 1.24$ g/cm^3 were determined by Atkins.[12] The amorphous order parameter f_a was calculated using the given values. The values f_a at different POYs are shown in Table IV.

Birefringence

The total birefringence Δn is usually interpreted as a superposition of amorphous and crystalline contributions:

$$\Delta n = x f_c \Delta n_c + (1 - x) f_a \Delta n_a$$

where x is the degree of crystallinity, f_c and f_a are the order parameters, for crystalline and amorphous parts, respectively, and Δn_c and Δn_a denote the specific birefringence for perfectly oriented crystalline and amorphous regions. The form birefringence is ignored.

x and f_c were determined by independent measurements using DSC and WAXS, respectively, and the values $\Delta n_c = 0.090$ and $\Delta n_a = 0.082$ were adapted with the order parameters of the sonic moduli. Table III shows the various values.

The order parameters $\langle P_2 \rangle$ obtained from NMR, WAXS, sonic propagation, and birefringence are given in Table IV. Figure 7 shows the $\langle P_2 \rangle$ values as a function of the spinning speed for the various techniques.

DISCUSSION

All orientational order measurements show the same effect, i.e., an approximately linear increase of the $\langle P_2 \rangle$ values at increasing spinning speeds.

Figure 5 TEM micrograph of a fully drawn yarn (FDY) spun at 600 m/min. The draw ratio was 4 : 5 (7400 : 1).

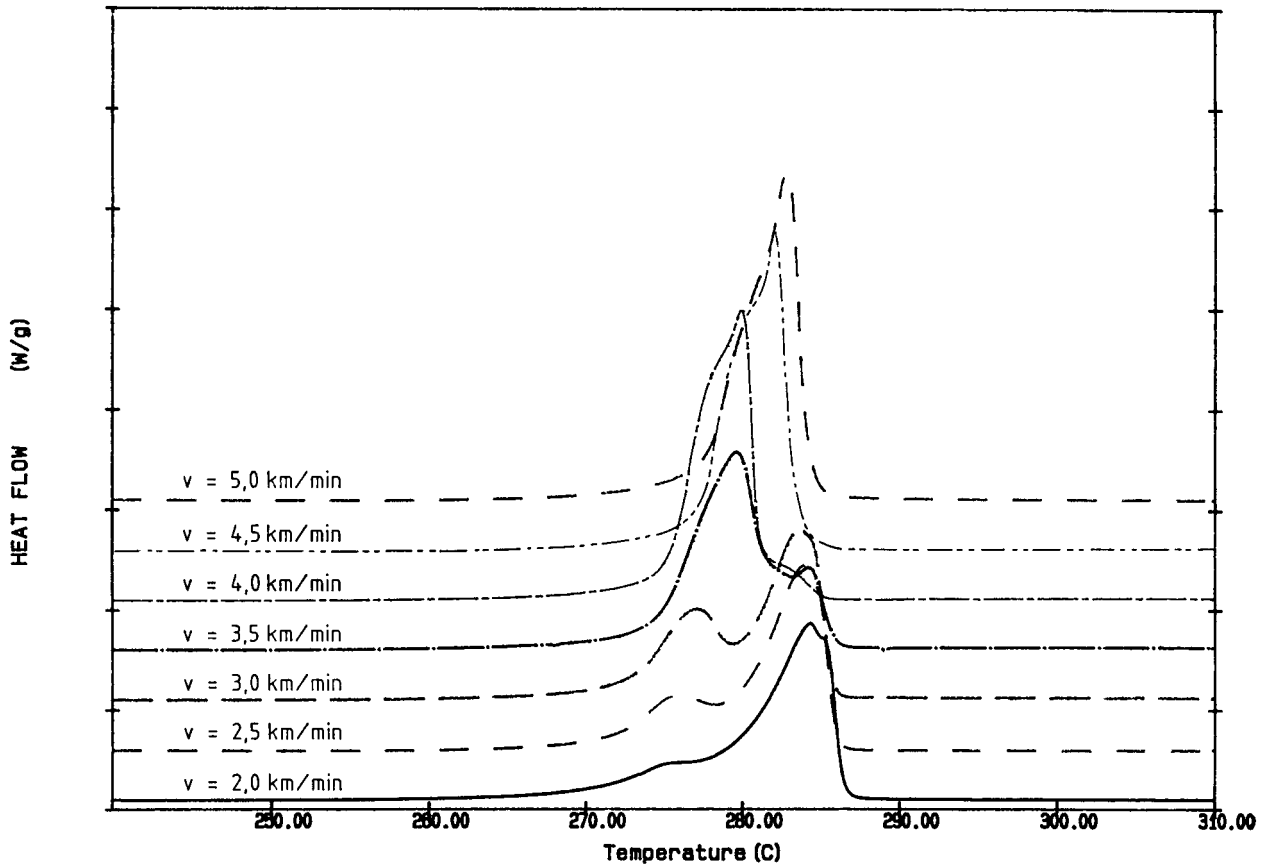

Figure 6 DSC thermograms of fibers spun at different spinning speeds.

The birefringence and sonic experiments yield values that are lower than the NMR values. The highest values were obtained by WAXS. This is due to the fact that the birefringence and sonic propagation order parameters represent the order in the amorphous regions, the NMR order parameters represent some average of the high crystalline and lower amorphous order and the WAXS measurements display the crystalline order.

The TEM pictures show that fibers spun in the range of speed from 2000 m/min to 3500 m/min possess at least partly a spherulitic structure. This agrees with the DSC measurements, when we assume that the melting of the spherulitic crystallites is responsible for the peak at the higher temperature. At spinning speeds higher than 3500 m/min spherulites are not longer visible in the TEM pictures and also the melting peak

Table III Various Parameters from DSC, Sonic Propagation, Birefringence, Tensile Tests, and WAXS Measurements

Yarn	v (km/min)	ΔH J/g	x	γ g/cm^3	t μs	E_{sonic} GPa	Δn	σ cN/dtex	D nm
POY	2.0	72.7	0.283	1.1783	187.1	3.03	0.0200	3.50	2.90
POY	2.5	73.2	0.285	1.1785	180.1	3.27	0.0250	3.40	3.08
POY	3.0	74.4	0.289	1.1789	175.4	3.45	0.0300	3.90	3.24
POY	3.5	80.7	0.314	1.1814	165.1	3.90	0.0340	4.10	3.58
POY	4.0	80.7	0.314	1.1814	157.5	4.29	0.0380	5.10	3.70
POY	4.5	83.6	0.325	1.1825	150.1	4.72	0.0430	5.30	3.93
POY	5.0	84.8	0.330	1.1830	146.7	4.95	0.0440	5.40	4.07
FDY	0.6	102.0	0.397	1.1897	124.8	6.87	0.0605	7.70	

Table IV The Order Parameters Determined from NMR, WAXS, Sonic Propagation, and Birefringence Experiments

		NMR			WAXS	Sonic	Δn
Yarn	v (km/min)	P_2 Crystalline + Amorphous	P_4	P_6	P_2 Crystalline	P_2 Amorphous	P_2 Amorphous
POY	2.0	0.45					
POY	2.5						
POY	3.0				0.66	0.15	0.22
POY	3.5	0.59	0.22				
POY	4.0				0.72	0.24	0.32
POY	4.5						
POY	5.0	0.73	0.51	0.34	0.77	0.38	0.39
FDY	0.6				0.85	0.51	0.61

in the DSC measurements at the higher temperature vanished. The spherulites cannot contribute to the orientational ordering because of their spherical structure. The disappearance of the spherulites with increased fiber spinning speed and at the same time an increase of the order parameters implies that the spherulitic crystal structure is replaced by crystalline structures, which are at least partly oriented parallel to the fiber axis due to the higher spinning speed.

The lower melting point in the DSC measurements, therefore, must be caused by orientationally induced crystallization. Both the orientation of the chains and the area of the first melting peak increase with increasing spinning speeds.

The fact that the first peak maximum of the DSC scans are shifted to higher temperatures at increasing spinning speeds means that the size of the crystals (D) grows (Table III) also. When the orientationally induced crystallization increases, the amorphous domains become more ordered, as the birefringence and sonic experiments show.

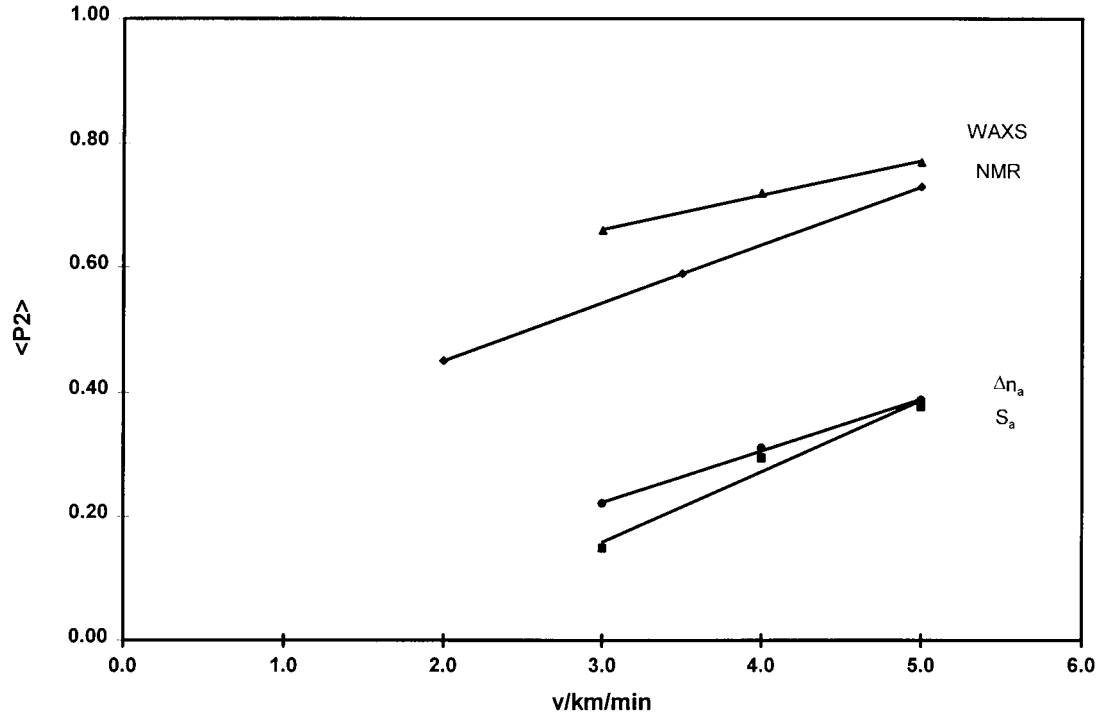

Figure 7 $<P_2>$ values as a function of the fiber spinning speed for WAXS, NMR, sonic, and birefringence measurements.

The TEM micrograph of the drawn fiber (Fig. 5) shows a fibril-like structure, with fibrils parallel to the fiber axis. This agrees with the orientation measurements, where the order parameters $\langle P_2 \rangle$ for the drawn fibers have the highest values.

CONCLUSION

The reported experiments, especially the TEM and DSC measurements, show the presence of two different crystalline morphologies in the textile fibers processed. The spherulite structure disappears in fibers that are spun at higher speeds. The determination of the orientational order and of the tenacity clearly shows the dependence on spinning speed and spin drawing. The differences between the amorphous order parameters of the POYs and FDYs are greater than the crystalline ones and explain the different levels of the tenacities (σ) for the POYs and FDYs (Table III).

The authors wish to thank Mr. C. Versluis, Mr. G. Krooshof, and Mr. St. Eltink from the DSM Research for stimulating discussions on the PA 4.6/6 spinning experiments and the structure formation of the spun PA 4.6/6 yarns. Also, the authors are grateful to the DSM Management for the financial support and the permission to publish the investigations.

REFERENCES

1. G. Krooshof, St. Eltink, and C. Versluis, TRI 63 rd Ann. Conf., Princeton, MA, 1993.
2. S. J. E. A. Eltink, S. De Boer, and J. A. H. M. Moonen, *NATO ASI Ser. C,* 555 (1993).
3. DSM brochure, Stanyl™. The polyamide 46 copolymer for yarns and fibres from DSM.
4. G. Schmack, H. Hofmann, R. Beyreuther, U. Müller, and D. Jehnichen, *Chem. Fibers Int.,* **45,** 475 (1995).
5. S. J. E. A. Eltink, personal report.
6. G. S. Harbison and H. W. Spiess, *Chem. Phys. Lett.,* **124,** 128 (1986).
7. G. S. Harbison, V.-D. Vogt, and H. W. Spiess, *J. Chem. Phys.,* **86,** 1206 (1987).
8. W. Gabriëlse, H. F. J. M. van Well, and W. S. Veeman, *Solid State NMR,* **6,** 231 (1996).
9. I. M. Ward, *Mechanical Properties of Solid Polymers,* Wiley–Interscience, London, 1971.
10. J. H. Dumbleton, *J. Polym. Sci. A-2,* **6,** 795 (1968).
11. S.-K. Hong, *Korea Polym. J.,* **3,** 48 (1995).
12. E. D. T. Atkins, M. Hill, S. K. Hong, A. Keller, and S. Organ, *Macromolecules,* **25,** 917 (1992).